Neurofilament Biophysics: from Structure to Biomechanics

Erika A. Ding[1] and Sanjay Kumar[1,2,3 *]

[1] Department of Chemical and Biomolecular Engineering, University of California, Berkeley, Berkeley, CA 94720, USA

[2] Department of Bioengineering, University of California, Berkeley, Berkeley, CA 94720, USA

[3] Department of Bioengineering and Therapeutic Sciences, University of California, San Francisco, San Francisco, CA 94158, USA

Running head: Neurofilament Biophysics

Abbreviations: NF, neurofilament; IDP, intrinsically disordered protein; NF-L, Neurofilament-Light; NF-M, Neurofilament-Medium; NF-H, Neurofilament-Heavy; IF, intermediate filament; PTM, post-translational modification; CMT, Charcot-Marie-Tooth disease; ALS, amyotrophic lateral sclerosis; AFM, atomic force microscopy; SCFT, self-consistent field theory

Keywords: neurofilaments, intrinsically disordered proteins, cytoskeleton, neuron biomechanics

Abstract

Neurofilaments (NFs) are multi-subunit, neuron-specific intermediate filaments consisting of a 10-nm diameter filament “core” surrounded by a layer of long intrinsically disordered protein (IDP) “tails”. NFs are thought to regulate axonal caliber during development and then stabilize the mature axon, with NF subunit misregulation, mutation, and aggregation featuring prominently in multiple neurological diseases. The field’s understanding of NF structure, mechanics, and function has been deeply informed by a rich variety of biochemical, cell biological, and mouse genetic studies spanning more than four decades. These studies have contributed much to our collective understanding of NF function in axonal physiology and disease. In recent years, however, there has been a resurgence of interest in NF subunit proteins in two new contexts: as potential blood- and cerebrospinal fluid-based biomarkers of neuronal damage, and as model IDPs with intriguing properties. Here we review established principles and more recent discoveries in NF structure and function. Where possible, we place these findings in the context of biophysics of NF assembly, interaction, and contributions to axonal mechanics.

Introduction

Neurofilaments (NFs) are intermediate filaments specific to neurons and serve as a major cytoskeletal component of large-diameter axons. Although classically viewed as space-filling axonal structures (Figure 1A), NFs are also found in the cell body and at synapses (Zheng *et al.*, 2003; Yuan *et al.*, 2015b) (Figure 1B). *In vivo*, NFs are obligate heteropolymers in that they are always composed of more than one type of subunit protein (Yuan *et al.*, 2017). In mammals, the five subunit proteins are Neurofilament-Light (NF-L), -Medium (NF-M), -Heavy (NF-H), α-internexin, and peripherin. These subunits assemble in a ratio that depends on species, developmental stage, neurodegenerative condition, age, localization in the neuron, and neuron type (Scott *et al.*, 1985; Kaplan *et al.*, 1990; Uchida *et al.*, 2004; Yuan *et al.*, 2006; Chinnakkaruppan *et al.*, 2009; Yuan *et al.*, 2012; Chen *et al.*, 2014).

The NF proteins share a general structure common to all intermediate filament (IF) proteins: a central α-helical rod domain is flanked by a short unstructured head domain and an unstructured tail domain of variable length (Figure 1C). Like other IF proteins, NF proteins assemble into filaments via their rod domains, which form coiled-coil dimers. These dimers assemble into tetramers, which associate into unit-length filaments and anneal end-to-end to form a long, 10-nm-diameter filament (Eldirany *et al.*,2021).

Although the NF proteins have long been of interest due to their role in axonal structure, the head and especially the tail domains have attracted renewed attention in recent years as functional intrinsically disordered proteins (IDPs). Disordered proteins lack a stably folded structure and instead dynamically sample a relatively large space of conformations. In recent years, IDPs have been increasingly implicated in the assembly of many intracellular condensates and membraneless organelles, cell signaling, and other protein-protein interactions (Martin and Holehouse, 2020; Borcherds *et al.*, 2021; Morris *et al.*, 2021; Uversky, 2021; Bondos *et al.*, 2022). In NFs, these repetitive, highly charged sequences also serve as a dynamic and tunable cytoskeletal building block.

The disordered tail domains physically protrude from the filament core, forming a bottlebrush-like structure (Willard and Simon, 1981; Hisanaga and Hirokawa, 1988) (Figure 1D). Because of their position at the periphery of the filament, the tail domains may govern inter-NF interactions depending on their

post-translational modifications (PTMs). The NF tail domains vary in phosphorylation capacity - the tail domains of NF-M and particularly NF-H are extensively phosphorylated *in vivo*, with the NF-H tail carrying ~50 phosphates (Yuan *et al.*, 2017). NF tail domain phosphorylation is regulated by a host of kinases and phosphatases (Veeranna *et al.*, 2011; Holmgren *et al.*, 2012; Lee *et al.*, 2014), and the degree of NF tail domain phosphorylation varies with age and with position along the length of the axon (Uchida *et al.*, 1999; Yuan *et al.*, 2015a). NFs can also undergo nitrosylation, glycosylation, and other PTMs, though the functions of these PTMs remain less well studied (Dong *et al.*, 1993; Snider and Omary, 2014; Petzold, 2022).

In recent years the NF proteins, especially NF-L, have become promising diagnostic biomarkers with the capacity to report on many neurodegenerative conditions (Lu *et al.*, 2015; Gaetani *et al.*, 2019; Lin *et al.*, 2019; Preische *et al.*, 2019; Rafii *et al.*, 2019; Lambertsen *et al.*, 2020; Zucchi *et al.*, 2020; Bittner *et al.*, 2021; Yuan and Nixon, 2021; Huehnchen *et al.*, 2022; Petzold, 2022). After axonal injury, the NF proteins are released from their canonical intracellular environment and end up in the blood or cerebrospinal fluid, where they can be measured as a proxy for neuronal damage. For example, a cohort of multiple sclerosis (MS) patients was found to have elevated serum NF-L relative to healthy controls (Disanto *et al.*, 2017). A recent meta-analysis of 31 studies further supported the diagnostic value of serum and plasma NF-L in MS and its subtypes and demonstrated predictive value for disease progression as quantified by the time to reach expanded disability status scale (EDSS) score > 4.0 (Ning and Wang, 2022). Nonetheless, diagnostic and prognostic applications of NF-L remain complicated, in part because baseline blood NF-L levels are affected by systemic factors such as body mass index, medication history, and especially age. Moreover, elevated NF-L is a somewhat nonspecific marker of neuronal damage and may reflect a variety of disease etiologies. Still, the relative stability of NF protein fragments enable their detection by single-molecule enzyme-linked immunosorbent assay. Patient autoantibodies recognizing NF proteins are also emerging biomarkers of neurodegeneration, and may complement the diagnostic value of the NF proteins themselves (Zmira *et al.*, 2020; Puentes *et al.*, 2021).

In addition to their translational potential, NFs represent an interesting biological system in which IDP conformational properties may directly contribute to whole-cell mechanics. Multiple excellent reviews have

discussed other aspects of NF biology including axonal transport, assembly, mutations in neurodegenerative disease, and potential as biomarkers (Didonna and Opal, 2019; Bomont, 2021; Eldirany *et al.*, 2021; Falzone *et al.*, 2021; Stone *et al.*, 2021; Yuan and Nixon, 2021, 2023; Petzold, 2022; Phillips *et al.*, 2023; Zhou *et al.*, 2023). In this review, we focus primarily on NFs as IDPs and regulators of neuronal biomechanics, tying together a selection of studies that have shed light on these structural yet unstructured proteins and their functions in forming filaments, maintaining axon caliber, and contributing to axon biomechanics.

Filament assembly and aggregation

Filament assembly

While the NF protein rod domains form the central filamentous core, filament assembly is strongly regulated by the disordered head domains. Analogously to other IFs such as vimentin (Herrmann *et al.*, 1996) and desmin (Sharma *et al.*, 2009), *in vitro* reconstitution shows that the head domain is required for NF-L filament assembly, as recombinant headless NF-L forms only short protofilaments when viewed by electron microscopy under standard filament assembly conditions (Heins *et al.*, 1993).

More recently, the molecular mechanism of NF-L head domain regulation has begun to be uncovered. Part of the head domain of NF-L can take on a transient beta strand-enriched conformation (Zhou *et al.*, 2021), which weakly binds other NF-L head domain proteins during the annealing stage of assembly (Figure 2A). This transient interaction is easily disrupted by phosphorylation (Figure 2B), and indeed, head domain phosphorylation has long been known to prevent reconstituted filament formation (Hisanaga *et al.*, 1990) and to control filament localization in neurons (Zheng *et al.*, 2003). Several NF-L head domain mutations associated with Charcot-Marie-Tooth disease (CMT) aberrantly strengthen the head domain self-interaction, preventing normal filament reconstitution *in vitro* and in SW13vim- cells (Sasaki *et al.*, 2006; Stone *et al.*, 2019; Zhou *et al.*, 2021, 2022). Interestingly, isolated NF-L head domains phase-separate *in vitro* into high-aspect-ratio or filamentous structures even without a rod domain, and CMT-associated mutations stabilize this structure even in multi-molar levels of urea (Zhou *et al.*, 2021). Less clear is how this potentially amyloid-like phase separation functions within the filamentous geometry of NF assembly and annealing. Indeed, very recent work on the structure of vimentin has

shown that the analogous disordered head domains form an amyloid-like fiber within the filament core (Eibauer *et al.*, 2023). It is possible that the distinct NF subunit head domains carry distinct phase separation properties, and it remains to be seen how these differences might regulate filament assembly.

In addition to filament formation, the head domain also regulates filament disassembly both *in vitro* and in cells (Hisanaga *et al.*, 1994; Giasson and Mushynski, 1998). Recent work has proposed that the cell regulates NF severing and transport by controlling phosphorylation of the NF protein head domains (Uchida *et al.*, 2023), as NF-L variants with phosphorylation-deficient head domains were severed significantly less frequently than phosphomimetic variants in cultured neurons (Figure 2C).

NF Bundles

Once formed, NFs are transported intermittently along microtubule tracks, but spend long periods of time "paused" as part of a cytoskeletal ultrastructure filling the axon (Wang *et al.*, 2000; Yuan *et al.*, 2015a). This model arises from observations of bidirectional, intermittent NF transport from time-lapse imaging of fluorescently labeled NFs in cultured neurons as well as transgenic mice (Wang *et al.*, 2000; Yan *et al.*, 2007; Boyer *et al.*, 2022). The NFs stationary at a given time have sometimes been referred to as a "bundle" formed of closely apposed filaments (Yamada *et al.*, 1971; Hirokawa *et al.*, 1984; Uchida *et al.*, 1999; Chen *et al.*, 2000; Yabe *et al.*, 2001) (Figure 2D). Centrally-situated bundles have been documented in cultured cell lines and neurons, as well as in regenerating nerve tissue from lamprey (Figure 2E) (Boumil *et al.*, 2018; Lee *et al.*, 2019).

Bundled NFs can be separated from nonbundled NFs by centrifuging tissue or cell homogenates over a sucrose cushion (Leterrier and Eyer, 1987; Leterrier *et al.*, 2009), enabling comparative studies. Bundled NFs are heavily phosphorylated at the NF-H tail domains, while the surrounding filaments are less phosphorylated (Kushkuley *et al.*, 2009; Boumil *et al.*, 2018). Studies in cultured cells have revealed that phosphorylation of the NF-H tail domain regulates the rate of NF bundling (Lee *et al.*, 2011, 2014; Vohnoutka *et al.*, 2017), and specifically that phosphorylation sites within the C-terminal ~190 amino acids of this tail domain are required for bundling (Chen *et al.*, 2000; Lee *et al.*, 2014).

NF bundles dissociate with the addition of EGTA (Kushkuley *et al.*, 2009), suggesting that multivalent cations are involved in crosslinking NFs into bundles. It has been proposed that crosslinking of tail-

phosphorylated NFs prevents their transport by kinesin (Yabe *et al.*, 2000; Kushkuley *et al.*, 2009; Shea and Lee, 2011; Sunil *et al.*, 2012), while nonphosphorylated NFs associate with kinesin and are more readily transported along microtubule tracks (Hisanaga and Hirokawa, 1990; Shea and Lee, 2011), though NF bundles do collapse upon application of actin- or microtubule-depolymerizing drugs (Lee *et al.*, 2019).

Aggregation

NFs can also be observed as large intracellular aggregates which characterize many neurodegenerative conditions including Alzheimer's disease, amyotrophic lateral sclerosis (ALS), Parkinson's disease, CMT, and neurofilament inclusion disease (Trojanowski and Lee, 1998; Uchikado *et al.*, 2006; Rudrabhatla *et al.*, 2011; Didonna and Opal, 2019). The molecular mechanisms by which filaments aggregate are complex and not well understood. Although NF-binding chemical moieties such as 3,3'-iminodipropionitrile (IDPN) or aluminum ions can cause general filament aggregation and neurotoxicity (Kushkuley *et al.*, 2010; Grande-Aztatzi *et al.*, 2020), disease models with NF aggregates have pointed to other causes such as altered NF subunit composition, disease-associated mutations, and misregulated clearance pathways.

One pathway driving filament aggregation is a misbalance in NF subunit stoichiometry, which has been principally studied in the context of ALS. Patient spinal cord samples show decreased NF-L, α-internexin, and peripherin mRNA levels, while NF-M and NF-H are unaffected (Wong *et al.*, 2000). Similarly, ALS-associated mutant SOD1 may destabilize NF-L mRNA, leading to aggregates which can be rescued by restoring NF-L expression (Chen *et al.*, 2014). Several miRNAs involved in ALS also differentially regulate the NF proteins, altering subunit stoichiometry (Campos-Melo *et al.*, 2018; Hawley *et al.*, 2019).

Moreover, overexpression of any of the NF proteins in mouse models can lead to NF accumulation, though not necessarily neuron loss. Comparison of mouse models and their effects are presented elsewhere (Didonna and Opal, 2019) (Table 2 in that publication). In order for subunit stoichiometry to support filament assembly, a minimum number of short-tailed NF proteins (α-internexin, peripherin, or especially NF-L) must be included. In reconstitution assays, NF-L/NF-M filaments become saturated at a

ratio of 37.5 mol% NF-M, and NF-L/NF-H filaments at 25 mol% NF-H (Jones and Safinya, 2008). This requirement may reflect similar steric constraints to those found in synthetic bottlebrush polymer self-assembly, where in a “grafting-to” approach the side-chain density can be limited by the crowding of long polymer chains (Verduzco *et al.*, 2015; Li *et al.*, 2021).

Disease-causing mutations such as those found in CMT may also cause NF aggregation. In a few cases, frameshift variants cause translation of an amyloidogenic sequence usually obscured in the 3’ UTR, causing aggregation (Rebelo *et al.*, 2016). However, many more reports have focused on other CMT-associated NF-L mutants, showing that these form aggregates in cultured cells (Zhai *et al.*, 2007; Lee *et al.*, 2008; Zhao *et al.*, 2017; Sainio *et al.*, 2018; Feliciano *et al.*, 2021). However, these assays frequently employ transient and uncontrolled overexpression of NF-L in systems with no other NF subunits. More recent work has shown that a variety of CMT-associated NF-L variants, while indeed unable to form homopolymeric filaments, are still able to incorporate into heteropolymeric filaments when co-expressed with other NF proteins such as NF-M or peripherin (Stone *et al.*, 2019). The authors suggest that CMT NF-L variants in heteropolymers *in vivo* may not aggregate due to improper filament assembly but rather due to aberrant protein-protein interactions, pointing to the importance of distinguishing filamentous from nonfilamentous aggregates in model systems.

Aggregation may also reflect misregulated NF degradation. NFs can be degraded by the proteasome via gigaxonin (Johnson-Kerner *et al.*, 2015) or TRIM2 (Balastik *et al.*, 2008), macroautophagy (Rao *et al.*, 2022), and calpain-mediated degradation after neuronal injury (Stys and Jiang, 2002). Disrupted degradation, such as in neurons lacking gigaxonin, results in a great increase in NF protein quantity and subsequent aggregation (Ganay *et al.*, 2011; Israeli *et al.*, 2016), potentially because kinesin is not recruited for NF transport (Renganathan *et al.*, 2023).

Whether NF-containing aggregates are themselves pathogenic or are simply byproducts of disease progression remains an unsettled question. Mouse models perturbing NF gene expression often result in aggregates, but only sometimes cause neurodegeneration (Eyer *et al.*, 1998; Perrot and Julien, 2011). The effects of NF-containing aggregates may depend on their location (Beaulieu *et al.*, 2000) – aggregates in the axon may block axonal transport and disrupt organelle localization (Straube-West *et al.*,

1996; Pérez-Ollé *et al.*, 2005; Zhai *et al.*, 2007; Lee *et al.*, 2012; Israeli *et al.*, 2016), while aggregates in the cell body are not predictive of neuropathic phenotype in NF overexpression cell culture or mouse models (Beaulieu *et al.*, 2000; Perrot and Julien, 2011).

Bundles and Aggregates

A comparison of bundling and aggregation may be useful in considering the molecular mechanisms of these processes. Bundling and aggregation both seem to involve a lateral association of large quantities of NFs, rather than improper filament assembly (Carter *et al.*, 1996), though aggregated filaments may have larger core diameters than wild type NFs when visualized by TEM (Uchikado *et al.*, 2006; Ganay *et al.*, 2011). Aggregates may be spherical in nature while bundles have high aspect ratio. Aggregates also tend to show “swirling” patterns of various filament orientations while non-aggregated NFs are more aligned with the axon (Ganay *et al.*, 2011) (Figure 2F), though single NFs in cultured neurons are observed to fold and bend, straightening out during transport (Fenn *et al.*, 2018).

Broadly, there remain fundamental unanswered questions around the molecular mechanisms of bundling and aggregation. For example, are NF “aggregates” physically crosslinked or entangled, or do they simply reflect local NF accumulations due to disrupted NF transport? How do inter-NF interactions control filament spacing, orientation, and aspect ratio, and how do these interactions relate to the usual dynamics of NF severing and annealing (Uchida *et al.*, 2013, 2023)? Structures described as bundles, filamentous aggregates, non-bundled filaments, and amorphous nonfilamentous aggregates are all observed in model systems, but can be difficult to distinguish by fluorescence microscopy alone. In this regard, mechanistic studies and quantification of NF spacing and orientation data from existing electron micrographs (Ganay *et al.*, 2011) may be useful.

Inter-filament interactions and axon caliber

The disordered tail domains are widely thought to mediate NF-NF interactions. NFs are generally found at a regular nearest-neighbor spacing on the order of ~30-50 nm in vivo (Table 1), and there has been much interest in understanding whether and how the tail domains maintain this spacing, particularly the relative contributions of the NF-M and NF-H tails. Two prevailing and non-mutually exclusive mechanisms by which NF tail interactions govern spacing include transient inter-NF ionic crosslinks and

entropic repulsion (Figure 3A). Both mechanisms are predicated on a model in which the intrinsically disordered NF protein tails protrude from the filament cores, forming a protein halo or brush around each filament that enables adjacent NFs to interact, and whose thickness determines inter-NF spacing.

Inter-NF crosslinks

Early evidence for NF crosslinks came from quick-freeze deep-etch electron microscopy of axonal cytoskeletons (Ellisman and Porter, 1980; Hirokawa, 1982), which revealed thin structures between adjacent filaments lost upon deleting the NF-M or NF-H tail domains (Chen *et al.*, 2000; Garcia *et al.*, 2003). These findings motivated the proposal that the NF tail domains directly participate in crosslinking of adjacent NFs, though inference of the strength or permanence of apparent crosslinks is complicated by the use of chemical fixation during sample preparation.

Divalent cations have also been implicated in this crosslinking mechanism. NF preparations purified from animal tissue form soft hydrogels in the presence of millimolar levels of magnesium or calcium ions. Some report that these hydrogels consist of both loose NFs and bundles of closely packed parallel NFs (Leterrier and Eyer, 1987; Leterrier *et al.*, 1996, 2009), while others do not report bundle formation (Yao *et al.*, 2010). This variation in structures suggests that there are multiple and potentially coexisting gel microstructures whose presence may depend on gelation conditions. Indeed, gelation is sensitive to many factors including co-purifying proteins, ionic strength, phosphorylation state, and ATP concentration in the preparation (Leterrier and Eyer, 1987; Eyer and Leterrier, 1988; Leterrier *et al.*, 1996, 2009; Gou *et al.*, 1998). Importantly, NFs denatured into their subunit proteins and reconstituted into filamentous form are incapable of gelation, even with divalent cations (Leterrier and Eyer, 1987), implying that divalent cations are necessary but not sufficient for gelation. The gelation mechanism may depend on factors lost during reconstitution such as another crosslinking protein, tail domain protein conformation (Leterrier and Eyer, 1987), physical force, or inter-filament entanglements due to ~μm-length reconstituted filaments being significantly shorter than native NFs (up to 100s of μm) (Uchida *et al.*, 2023).

Instead of using intact filaments purified from tissue, NF hydrogels can also be formed by reconstitution of purified NF subunit proteins into filaments by dialysis, then ultracentrifugation with divalent cations (Jones and Safinya, 2008; Beck *et al.*, 2010b). This method forms hydrogels which,

depending on salinity and protein stoichiometry, can take on birefringent nematic, isotropic, or opaque liquid crystalline phases (Deek *et al.*, 2013). In a nematic phase, long particles (NFs) are relatively aligned, as opposed to an isotropic phase in which filament orientation is random (Figure 3B). The opaque phase, which corresponds to crosslinked bundles of NFs, was only observed at very low ionic strengths. In the vicinity of physiological ionic strength the nematic phase is predominant, with NFs aligned and relatively evenly spaced (Deek *et al.*, 2013, 2016).

The spacing between filaments within these gels can be measured by small-angle X-ray scattering (SAXS), with or without molecular crowders to control osmotic pressure (Beck *et al.*, 2010b). Beyond a critical osmotic pressure threshold around 10 kPa, the filaments irreversibly compact together, with NF-NF spacing reduced from >60 nm to ~40 nm. The reconstituted filament system allows control over subunit composition, removal of proteins that co-purify with tissue-derived NFs, and a detailed study of how subunit composition impacts NF-NF spacing. The results are complex, interdependent, and not always in agreement with other models (Table 1).

These data led to the “handshake” model of crosslinking between NF tails (Beck *et al.*, 2010b), which assigns an energetic contribution for pairwise residue interactions based on charge and hydrophobicity. This model has identified some regions of NF-M and NF-H tails that may enable hydrophobic and ionic crosslinks, respectively. Though the handshake model does not predict attractive interactions between NF-L tails, an *in vitro* study has shown that gold nanoparticles coated with NF-L tail constructs aggregate in the presence of divalent cations, suggesting an additional ionic crosslinking mechanism involving NF-L tails (Pregent *et al.*, 2015).

Entropic repulsion

The entropic repulsion model (Brown and Hoh, 1997) was inspired by atomic force microscopy (AFM) which revealed a region around native NFs from which other proteins are excluded (Figure 3C). The size of this region depends on the solution ionic strength, filament composition, phosphorylation state, and presence of divalent cations (Kumar and Hoh, 2004). In the entropic model, confinement would restrict the large set of tail domain conformations and is thus entropically unfavorable, resulting in an inter-filament repulsive force. This “entropic brush” model is in analogy to polymer brushes, synthetic

polymer systems where one side of each polymer (tail domain) is tethered to a surface (filament core) and the other end is free.

Quantitative analysis of axonal electron micrographs, together with Monte Carlo simulations under varying NF-NF pair potentials, show that purely repulsive inter-filament interactions could recapitulate the observed NF spacings seen *in vivo* (Kumar *et al.*, 2002). In general, theoretical and computational approaches have proven particularly well suited to study protein conformations within NF brushes, which are difficult to access experimentally. Several groups have performed Monte Carlo simulations using models of NF tails coarse-grained at the amino acid level and grafted to a cylindrical core. These studies have revealed that at low salt and without tail phosphorylation, the NF-L tail forms a sub-brush layer near the filament core (Stevenson *et al.*, 2011) (Figure 3D). The composition of this sub-brush may govern the more extended conformations of the NF-M and phosphorylated NF-H tails (Leermakers and Zhulina, 2010). Filaments pushed together will sometimes repel, but can overlap especially at close packing and significant amounts of salt (Jayanthi *et al.*, 2013). At high ionic strength, simulations have found opposite effects of NF-H and NF-M (Chang *et al.*, 2009; Kim *et al.*, 2011; Lee *et al.*, 2013) (Table 1).

Self-consistent field theory (SCFT) is also well suited to studying polymer brushes, and has also been applied to the NF tails (Zhulina and Leermakers, 2009; Yokokura *et al.*, 2023). SCFT applies a mean-field approximation to a coarse-grained model of the NF tails, using the sequence-dependent charge and hydrophobicity within each protein chain to determine the location profiles of amino acid monomers making up the brush structure (Figure 3E). SCFT studies have aligned well with the computational observation that NF-L forms a sub-brush (Leermakers and Zhulina, 2010), with the longer NF-M and NF-H tails protruding, especially when phosphorylated. However, in the SCFT model, NF-M tends to set a taller brush height than NF-H (Zhulina and Leermakers, 2007, 2009, 2010) (Table 1). This model predicts that the NF-L sub-brush electrostatically repels or attracts the NF-H tail depending on whether the latter is phosphorylated (Zhulina and Leermakers, 2009). Substituting α-internexin for NF-L reduces the repulsive force on NF-M and NF-H tails, leading to overall shorter brush heights (Leermakers and Zhulina, 2010) (Table 1).

Grafting purified NF tail proteins to a solid support is a powerful reconstitution paradigm that allows assembly of NF tails in their physiological orientation and direct measurement of the resulting brush thickness by AFM. In one set of studies, NF-H tail domains were expressed in *E. coli* and grafted to a functionalized substrate in an end-directed fashion via an engineered cysteine, creating a brush of similar grafting density to a native neurofilament tail brush (Srinivasan *et al.*, 2014). At neutral pH, a purely NF-H tail brush takes on a collapsed conformation. These brushes can also be phosphorylated by purified kinases *in vitro*; upon phosphorylation, the NF-H tail brush expands significantly, though less dramatically at physiological ionic strength (Lei *et al.*, 2018). As expected for a polyelectrolyte brush, divalent cations collapse the brush at lower concentrations than monovalent cations (Lei *et al.*, 2018).

Other work has examined how the protein sequence determines the conformational ensembles taken by the tail domains. Using SAXS and time-resolved Förster resonance energy transfer (trFRET), Koren et al. showed that the C-terminal region of the NF-L tail may loop back to interact with more N-terminal segments of the sequence (Koren *et al.*, 2023). Loops have also been noted to form in Monte Carlo simulations of NF-M and NF-H tails (Chang *et al.*, 2009). Molecular dynamics simulations showed that salt bridges within the NF-H tail can make small loops, which help the tail stay within the brush (Adiga and Brenner, 2010). These loops are disrupted upon phosphorylation enabling a dramatic expansion of the chain, though this work considered the context of a dilute untethered protein rather than a crowded brush. NF-H tail loops are also consistent with single-molecule force spectroscopy data (Aranda-Espinoza *et al.*, 2002), though in this technique it is challenging to ensure pulling of only single protein molecules without experimental controls such as covalent surface linking or recombinant fingerprint domains (Yang *et al.*, 2020).

Recent experimental work has also examined the conformation of a fragment of the NF-M tail which has blocks of positive and negative charge of various lengths (Bianchi *et al.*, 2020). The authors shuffled the charged residues to be more evenly spaced and found that the charge-shuffled protein takes on a more expanded conformation than the wild type. While it is not clear whether this sequence-conformation relationship would also hold for the full length NF-M tail in the context of a crowded brush, Monte Carlo simulations in the brush context support the idea that a positively charged block near the center of the

NF-M tail remains pinned to the sub-brush, with more C-terminal negatively charged blocks protruding further and contributing to brush height (Chang *et al.*, 2009; Jeong *et al.*, 2016). In that case, an evenly shuffled charge distribution could un-pin the central charged block and expand the protein.

Axon caliber

NFs are important in developing axons of large caliber, which is critical for conduction velocity. NFs in large-caliber axons can significantly outnumber microtubules (Hoffman *et al.*, 1984), and caliber is reduced in multiple axonal-NF-deficient mouse models (Eyer and Peterson, 1994; Zhu *et al.*, 1997) and in NF-L-nonsense quail (Yamasaki *et al.*, 1991; Ohara *et al.*, 1993). The relative expression levels of the NF proteins are important to support caliber increases, as various NF protein knockout and overexpression mouse models have resulted in decreased calibers while only simultaneous overexpression of NF-L and either NF-M or NF-H resulted in increased caliber (Marszalek *et al.*, 1996; Xu *et al.*, 1996; Meier *et al.*, 1999; Perrot and Julien, 2011). However, knockout mouse models used to study this effect can potentially produce compensatory changes in expression of other NF proteins or cytoskeletal elements such as microtubules, making interpretation challenging (Elder *et al.*, 1998; Rao *et al.*, 1998; Jacomy *et al.*, 1999; Yuan *et al.*, 2006).

Gene replacement mouse models have shown that deleting the NF-M tail domain results in reduced axonal caliber and more NF clustering, indicating the importance of this protein domain for caliber maintenance (Garcia *et al.*, 2003). However, replacement of the NF-M tail phosphorylation sites with nonphosphorylatable alanine residues produces effectively no change in spacing or caliber (Garcia *et al.*, 2009). Similar models have also shown that deleting the NF-H tail surprisingly does not affect caliber, inter-NF spacing, or NF transport rate, though NF-M tail phosphorylation was upregulated in response (Rao *et al.*, 2002, 2003).

NF spacing and axon caliber were originally thought to be directly related; however, genetically altered animal models have exhibited changes in axon caliber without changes in NF-NF spacing (Elder *et al.*, 1998; Barry *et al.*, 2012), as well as large changes in spacing without correspondingly large changes in caliber (Xu *et al.*, 1996). The amount of correctly assembled heteropolymeric NFs in the axon does seem to be an important factor in determining axon caliber. Myelin-dependent signaling via myelin-

associated glycoprotein locally regulates NF phosphorylation in internodes and subsequent changes in NF transport rates (De Waegh *et al.*, 1992; Yin *et al.*, 1998; Monsma *et al.*, 2014). However, the mechanism connecting NF content and axon caliber growth remains unclear (De Waegh *et al.*, 1992; Yin *et al.*, 1998; Garcia *et al.*, 2003).

Cell mechanics and cytoskeleton

NFs as a structural element in the axon

As some intermediate filaments are cell-type specific, IFs have been hypothesized to support cell-specific mechanical needs. NFs have been thought to mechanically support the thin and fragile axon (Kornreich *et al.*, 2016) as part of the larger axonal cytoskeleton (Figure 4A). This biomechanical function remains incompletely understood in the full complexity of a neuron. However, insights may be gained by examining the body of *in vitro* work on the mechanical properties of single NFs and NF-based materials.

Along with other IFs, single NFs are highly stretchable up to 3.4 times their original length in axial tension (Kreplak *et al.*, 2005). Upon stretching, single NFs also thin dramatically, which may be due to partial filament unraveling (Wagner *et al.*, 2007), or partial unfolding of the rod domain proteins as is the case for vimentin (Block *et al.*, 2018). NF-L-only filaments are less mechanically robust than native filaments (Brown *et al.*, 1998), but whether this is due to the filament reconstitution process or subunit composition itself is unclear. Single filaments can also be characterized by their persistence length L_p, which is a measure of filament stiffness. While L_p is >1 mm for microtubules and ~10 μm for F-actin, intermediate filaments tend to be much more flexible, with L_p ~ 100s of nanometers (Dalhaimer *et al.*, 2005; Wagner *et al.*, 2007). For NFs, L_p has been measured by AFM to be between 100-450 nm (Dalhaimer *et al.*, 2005; Beck *et al.*, 2010a). Notably, the mechanics of isolated NF bundles have not been studied.

NF hydrogel mechanical properties have been more thoroughly characterized. Rheological studies have measured storage and loss moduli, which respectively reflect a material's ability to store and internally dissipate applied stress. Tissue-prepared native NF hydrogels are very soft with shear storage moduli of ~1-100 Pa. These gels also demonstrate strain stiffening up to 200 Pa, are capable of stress

relaxation (Leterrier *et al.*, 1996), and can self-heal several times after mechanical disruption (Leterrier and Eyer, 1987).

Several studies have explored the mechanism by which NF hydrogels resist stress. The storage modulus of these gels is much greater than the loss modulus, reflecting a crosslinked solid hydrogel (Yao *et al.*, 2010). The hydrogel storage modulus depends directly on the concentration of Mg2+, implicating divalent cations in the crosslinking mechanism. Yao et al. suggest that the hydrogel elasticity derives from the entropic penalty of stretching single NFs, which due to their low persistence length are semiflexible between crosslink sites. In this work and a related study (Lin *et al.*, 2010) the authors calculated mesh sizes on the order of a few hundred nanometers and did not observe bundling by optical microscopy, while other studies of similar NF preparations measured mesh sizes on the order of micrometers and correspondingly observed bundles by electron microscopy (Leterrier and Eyer, 1987; Leterrier *et al.*, 1996; Rammensee *et al.*, 2007). Interestingly, significant amounts of glycerol or sucrose are also required for gelation, suggesting the importance of crowding and osmotic pressure for NF-NF crosslinking (Leterrier *et al.*, 1996). Gelation is also slowed significantly and gels are significantly softer at physiological levels of monovalent salt, which is not present at high concentrations in the standard preparation buffer (Leterrier and Eyer, 1987; Rammensee *et al.*, 2007).

Reconstituted NF hydrogels, where filaments can be aligned, reconstituted, and controlled more precisely, generally exhibit much stiffer storage moduli of hundreds to several thousands of Pa (Deek *et al.*, 2013), though they can be softened somewhat with monovalent salt. Measuring the effect of osmotic pressure on filament spacing enables calculating the bulk modulus, another measure of the stiffness of a material (Malka-Gibor *et al.*, 2017). Phosphorylation of NF-H increased the hydrogel bulk modulus, suggesting that the effect of NF-H phosphorylation may be mechanical rather than structural (Malka-Gibor *et al.*, 2017). This suggestion has also arisen in Monte Carlo simulations (Kim *et al.*, 2011). However, the specific mechanism – for example, due to steric or osmotic swelling effects – remains unclear.

In living cells, of course, the picture is more complicated; only a few studies have quantified contributions of NFs to cell-scale mechanical properties. Direct measurements of axonal mechanics by magnetic tweezer creep tests have demonstrated that NFs generally contribute to stiffness of the cell

body and promote axonal viscoelasticity, while microtubules promote elastic character in the axon (Grevesse *et al.*, 2015) (Figure 4B). Another previous study indicated that NFs contribute significantly to neurite stiffness, though not as much as microtubules (Ouyang *et al.*, 2013). Notably, the effect of NFs in both studies was assessed by treating cells with chemical agents directed against intermediate filaments such as acrylamide and IDPN, which may have many off-target effects at moderate levels and are cytotoxic at higher levels.

Crosslinking proteins and cytoskeletal crosstalk

NF ultrastructure may be remodeled by crosslinking proteins. In a pulldown assay using the NF-L head domain as "bait" (Zhou *et al.*, 2021), many cytoskeleton-related proteins were enriched from mouse brain lysate including other NF proteins, actin, spectrin, tubulin, dynein, and kinesin. Dynein and kinesin are known to link NFs to the microtubule network, enabling NF transport (Shah *et al.*, 2000; Yabe *et al.*, 2000; Xia *et al.*, 2003; Wagner *et al.*, 2004; Francis *et al.*, 2005; He *et al.*, 2005; Kushkuley *et al.*, 2009; Uchida *et al.*, 2009). NFs are also a negative regulator of microtubule dynamics (Bocquet *et al.*, 2009; Yadav *et al.*, 2016), possibly in an aggregation-dependent manner (Kurup *et al.*, 2018). This finding might shed light on compensation between MTs and NFs in NF-deficient models. The contrast between the stable structural NF core and the dynamic, disordered outer layer stands in structural analogy to microtubules and their dynamic surrounding layer of C-terminal tails and often disordered MAPs (Bodakuntla *et al.*, 2019), which may serve as an alternative neuronal cytoskeleton in the absence of NFs (Prokop, 2020).

Other putative crosslinking proteins include BPAG1-n, a neuronal isoform of BPAG1 whose knockout causes perikaryal NF accumulation in mice (Yang *et al.*, 1996), and plectin, which binds other IFs at the rod domain (Potokar and Jorgačevski, 2021; Wiche, 2021). Plectin isoform P1c has been observed to colocalize with NFs *in vivo* (Potokar and Jorgačevski, 2021).

Conclusion

NFs are a complex, tunable, and dynamic structural system within the neuron, with properties enabled by a combination of ordered and disordered protein regions. The exciting IDP physics unfolding in the NF-L head domain invites comparison to other NF subunit head domains, as they might

differentially regulate filament formation. In cell mechanics, many mechanisms remain unknown, for example how NF abundance contributes to axon caliber; how divalent cations mediate NF bundling; the mechanism of NF aggregation; and whether the distinct subunit proteins, phosphorylation, and NF ultrastructure affect axon mechanical properties. Many of these mechanistic questions will benefit from a deeper understanding of the relevant IDP physics, especially of the NF tail domains.

Understanding the biophysical function of NFs and their disordered domains may facilitate aspects of biomarker development. Work exploring the prognostic value of different NF subunits or fragments and their phosphorylation levels, or accounting for aggregation kinetics in biofluids (Lu *et al.*, 2011; Adiutori *et al.*, 2018; Budelier *et al.*, 2022; Petzold, 2022), could be informed by a deeper understanding of the biophysics underlying NF protein stoichiometry, phosphorylation, and aggregation. For example, whereas NF-L is a somewhat nonspecific marker of neuronal damage, there could be value in developing more precise NF subunit-based biomarkers that reflect specific mechanisms of damage.

The disordered NF domains are also a unique model system for understanding IDP function more broadly. In particular, the extensive phosphorylation and high proline content in the NF-H tail domain is quite unusual within the proteome and poses an opportunity to explore multi-phosphorylated and proline-dependent conformational ensembles, both of which are current frontiers within IDP research. Further, disordered NF domains demonstrate the effects of system geometry, with the head domains contributing to filamentous assembly and the tail domains tethered to the core in a cylindrical protein brush. A protein brush geometry is also found in the disordered proteins of the nuclear pore complex, enabling comparison of these to other dense IDP assemblies and condensates.

Acknowledgements

This work was supported by NIH R01GM122375 to SK and the National Science Foundation Graduate Research Fellowship under Grant No. DGE 2146752 to EAD.

References

Adiga, SP, and Brenner, DW (2010). Molecular basis for neurofilament heavy chain side arm structure modulation by phosphorylation. J Phys Chem C 114, 5410–5416.

Adiutori, R, Aarum, J, Zubiri, I, Bremang, M, Jung, S, Sheer, D, Pike, I, and Malaspina, A (2018). The proteome of neurofilament-containing protein aggregates in blood. Biochem Biophys Rep 14, 168–177.

Aranda-Espinoza, H, Carl, P, Leterrier, JF, Janmey, P, and Discher, DE (2002). Domain unfolding in neurofilament sidearms: Effects of phosphorylation and ATP. FEBS Lett 531, 397–401.

Balastik, M, Ferraguti, F, Pires-da Silva, A, Lee, T, Alvarez-Bolado, G, Lu, K, and Gruss, P (2008). Deficiency in ubiquitin ligase TRIM2 causes accumulation of neurofilament light chain and neurodegeneration. Proc Natl Acad Sci 105, 12016–12021.

Barry, DM, Stevenson, W, Bober, BG, Wiese, PJ, Dale, JM, Barry, GS, Byers, NS, Strope, JD, Chang, R, Schulz, DJ, *et al.* (2012). Expansion of neurofilament medium C terminus increases axonal diameter independent of increases in conduction velocity or myelin thickness. J Neurosci 32, 6209–6219.

Beaulieu, JM, Jacomy, H, and Julien, JP (2000). Formation of intermediate filament protein aggregates with disparate effects in two transgenic mouse models lacking the neurofilament light subunit. J Neurosci 20, 5321–5328.

Beck, R, Deek, J, Choi, MC, Ikawa, T, Watanabe, O, Frey, E, Pincus, P, and Safinya, CR (2010a). Unconventional Salt Trend from Soft to Stiff in Single Neurofilament Biopolymers. Langmuir 26, 18595–18599.

Beck, R, Deek, J, Jones, JB, and Safinya, CR (2010b). Gel-expanded to gel-condensed transition in neurofilament networks revealed by direct force measurements. Nat Mater 9, 40–46.

Bianchi, G, Longhi, S, Grandori, R, and Brocca, S (2020). Relevance of electrostatic charges in compactness, aggregation, and phase separation of intrinsically disordered proteins. Int J Mol Sci 21, 1–30.

Bittner, S, Oh, J, Havrdová, EK, Tintoré, M, and Zipp, F (2021). The potential of serum neurofilament as biomarker for multiple sclerosis. Brain 144, 2954–2963.

Block, J, Witt, H, Candelli, A, Danes, JC, Peterman, EJG, Wuite, GJL, Janshoff, A, and Köster, S (2018). Viscoelastic properties of vimentin originate from nonequilibrium conformational changes. Sci Adv 4.

Bocquet, A, Berges, R, Frank, R, Robert, P, Peterson, A, and Eyer, J (2009). Neurofilaments bind tubulin and modulate its polymerization. J Neurosci 29, 11043–11054.

Bodakuntla, S, Jijumon, AS, Villablanca, C, Gonzalez-Billault, C, and Janke, C (2019). Microtubule-Associated Proteins: Structuring the Cytoskeleton. Trends Cell Biol 29, 804–819.

Bomont, P (2021). The dazzling rise of neurofilaments: Physiological functions and roles as biomarkers. Curr Opin Cell Biol, 1–11.

Bondos, SE, Dunker, AK, and Uversky, VN (2022). Intrinsically disordered proteins play diverse roles in cell signaling. Cell Commun Signal 20, 20.

Borcherds, W, Bremer, A, Borgia, MB, and Mittag, T (2021). How do intrinsically disordered protein regions encode a driving force for liquid–liquid phase separation? Curr Opin Struct Biol 67, 41–50.

Boumil, EF, Vohnoutka, R, Lee, S, Pant, H, and Shea, TB (2018). Assembly and turnover of neurofilaments in growing axonal neurites. Biol Open 7.

Boyer, NP, Julien, J-P, Jung, P, and Brown, A (2022). Neurofilament Transport Is Bidirectional In Vivo. eNeuro 9, ENEURO.0138-22.2022.

Brown, HG, and Hoh, JH (1997). Entropic Exclusion by Neurofilament Sidearms: A Mechanism for Maintaining Interfilament Spacing. Biochemistry 36, 15035–15040.

Brown, Troncoso, and Hoh (1998). Neurofilament-L homopolymers are less mechanically stable than native neurofilaments. J Microsc 191, 229–237.

Budelier, MM, He, Y, Barthelemy, NR, Jiang, H, Li, Y, Park, E, Henson, RL, Schindler, SE, Holtzman, DM, and Bateman, RJ (2022). A map of neurofilament light chain species in brain and cerebrospinal fluid and alterations in Alzheimer's disease. Brain Commun 4, 1–12.

Campos-Melo, D, Hawley, ZCE, and Strong, MJ (2018). Dysregulation of human NEFM and NEFH mRNA stability by ALS-linked miRNAs. Mol Brain 2018 111 11, 1–9.

Carter, JE, Gallo, J-M, Anderson, VER, Anderton, BH, and Robertson, J (1996). Aggregation of Neurofilaments in NF-L Transfected Neuronal Cells: Regeneration of the Filamentous Network by a Protein Kinase C Inhibitor. J Neurochem 67, 1997–2004.

Chang, R, Kwak, Y, and Gebremichael, Y (2009). Structural Properties of Neurofilament Sidearms: Sequence-Based Modeling of Neurofilament Architecture. J Mol Biol 391, 648–660.

Chen, H, Qian, K, Du, Z, Cao, J, Petersen, A, Liu, H, Blackbourn, LW, Huang, CL, Errigo, A, Yin, Y, *et al.* (2014). Modeling ALS with iPSCs reveals that mutant SOD1 misregulates neurofilament balance in motor neurons. Cell Stem Cell 14, 796–809.

Chen, J, Nakata, T, Zhang, Z, and Hirokawa, N (2000). The C-terminal tail domain of neurofilament protein-H (NF-H) forms the crossbridges and regulates neurofilament bundle formation. J Cell Sci 113, 3861–3869.

Chinnakkaruppan, A, Das, S, and Sarkar, PK (2009). Age related and hypothyroidism related changes on the stoichiometry of neurofilament subunits in the developing rat brain. Int J Dev Neurosci 27, 257–261.

Dalhaimer, P, Wagner, OI, Leterrier, JF, Janmey, PA, Aranda-Espinoza, H, and Discher, DE (2005). Flexibility transitions and looped adsorption of wormlike chains. J Polym Sci Part B Polym Phys 43, 280–286.

De Waegh, SM, Lee, VM-Y, and Brady, ST (1992). Local modulation of neurofilament phosphorylation, axonal caliber, and slow axonal transport by myelinating Schwann cells. Cell 68, 451–463.

Deek, J, Chung, PJ, Kayser, J, Bausch, AR, and Safinya, CR (2013). Neurofilament sidearms modulate parallel and crossed-filament orientations inducing nematic to isotropic and re-entrant birefringent hydrogels. Nat Commun 4, 1–10.

Deek, J, Chung, PJ, and Safinya, CR (2016). Neurofilament networks: Salt-responsive hydrogels with sidearm-dependent phase behavior. Biochim Biophys Acta - Gen Subj 1860, 1560–1569.

Didonna, A, and Opal, P (2019). The role of neurofilament aggregation in neurodegeneration: Lessons from rare inherited neurological disorders. Mol Neurodegener 14, 1–10.

Disanto, G, Barro, C, Benkert, P, Naegelin, Y, Schädelin, S, Giardiello, A, Zecca, C, Blennow, K, Zetterberg, H, Leppert, D, *et al.* (2017). Serum Neurofilament light: A biomarker of neuronal damage in multiple sclerosis. Ann Neurol 81, 857–870.

Dong, DL, Xu, ZS, Chevrier, MR, Cotter, RJ, Cleveland, DW, and Hart, GW (1993). Glycosylation of mammalian neurofilaments. Localization of multiple O-linked N-acetylglucosamine moieties on neurofilament polypeptides L and M. J Biol Chem 268, 16679–16687.

Eibauer, M, Weber, MS, Kronenberg-Tenga, R, Beales, CT, Boujemaa-Paterski, R, Turgay, Y, Sivagurunathan, S, Kraxner, J, Köster, S, Goldman, RD, *et al.* (2023). Vimentin filaments integrate low complexity domains in a highly complex helical structure. *bioRxiv* 2023.05.22.541714. doi: 10.1101/2023.05.22.541714

Elder, GA, Friedrich, VL, Kang, C, Bosco, P, Gourov, A, Tu, P-H, Zhang, B, Lee, VM-Y, and Lazzarini, RA (1998). Requirement of Heavy Neurofilament Subunit in the Development of Axons with Large Calibers. J Cell Biol 143, 195–205.

Eldirany, SA, Lomakin, IB, Ho, M, and Bunick, CG (2021). Recent insight into intermediate filament structure. Curr Opin Cell Biol 68, 132–143.

Ellisman, M, and Porter, K (1980). Microtrabecular structure of the axoplasmic matrix: visualization of cross-linking structures and their distribution. J Cell Biol 87, 464–479.

Eyer, J, Cleveland, DW, Wong, PC, and Peterson, AC (1998). Pathogenesis of two axonopathies does not require axonal neurofilaments. Nat 1998 3916667 391, 584–587.

Eyer, J, and Leterrier, JF (1988). Influence of the phosphorylation state of neurofilament proteins on the interactions between purified filaments in vitro. Biochem J 252, 655–660.

Eyer, J, and Peterson, A (1994). Neurofilament-deficient axons and perikaryal aggregates in viable transgenic mice expressing a neurofilament-β-galactosidase fusion protein. Neuron 12, 389–405.

Falzone, YM, Russo, T, Domi, T, Pozzi, L, Quattrini, A, Filippi, M, and Riva, N (2021). Current application of neurofilaments in amyotrophic lateral sclerosis and future perspectives. Neural Regen Res 16, 1985.

Feliciano, CM, Wu, K, Watry, HL, Marley, CBE, Ramadoss, GN, Ghanim, HY, Liu, AZ, Zholudeva, LV, McDevitt, TC, Saporta, MA, *et al.* (2021). Allele-Specific Gene Editing Rescues Pathology in a Human Model of Charcot-Marie-Tooth Disease Type 2E. Front Cell Dev Biol 9, 723023.

Fenn, JD, Monsma, PC, and Brown, A (2018). Axonal neurofilaments exhibit frequent and complex folding behaviors. Cytoskeleton 75, 258–280.

Francis, F, Roy, S, Brady, ST, and Black, MM (2005). Transport of neurofilaments in growing axons requires microtubules but not actin filaments. J Neurosci Res 79, 442–450.

Gaetani, L, Blennow, K, Calabresi, P, Filippo, MD, Parnetti, L, and Zetterberg, H (2019). Neurofilament light chain as a biomarker in neurological disorders. J Neurol Neurosurg Psychiatry 90, 870–881.

Ganay, T, Boizot, A, Burrer, R, Chauvin, JP, and Bomont, P (2011). Sensory-motor deficits and neurofilament disorganization in gigaxonin-null mice. Mol Neurodegener 6, 25.

Garcia, ML, Lobsiger, CS, Shah, SB, Deerinck, TJ, Crum, J, Young, D, Ward, CM, Crawford, TO, Gotow, T, Uchiyama, Y, *et al.* (2003). NF-M is an essential target for the myelin-directed “outside-in” signaling cascade that mediates radial axonal growth. J Cell Biol 163, 1011–1020.

Garcia, ML, Rao, MV, Fujimoto, J, Garcia, VB, Shah, SB, Crum, J, Gotow, T, Uchiyama, Y, Ellisman, M, Calcutt, NA, *et al.* (2009). Phosphorylation of highly conserved neurofilament medium KSP repeats is not required for myelin-dependent radial axonal growth. J Neurosci 29, 1277–1284.

Giasson, BI, and Mushynski, WE (1998). Intermediate Filament Disassembly in Cultured Dorsal Root Ganglion Neurons Is Associated with Amino-Terminal Head Domain Phosphorylation of Specific Subunits. J Neurochem 70, 1869–1875.

Gou, JP, Gotow, T, Janmey, PA, and Leterrier, JF (1998). Regulation of neurofilament interactions in vitro by natural and synthetic polypeptides sharing Lys-Ser-Pro sequences with the heavy neurofilament subunit NF-H: Neurofilament crossbridging by antiparallel sidearm overlapping. Med Biol Eng Comput 36, 371–387.

Grande-Aztatzi, R, Formoso, E, Mujika, JI, de Sancho, D, and Lopez, X (2020). Theoretical characterization of Al(III) binding to KSPVPKSPVEEKG: Insights into the propensity of aluminum to interact with key sequences for neurofilament formation. J Inorg Biochem 210, 111169.

Grevesse, T, Dabiri, BE, Parker, KK, and Gabriele, S (2015). Opposite rheological properties of neuronal microcompartments predict axonal vulnerability in brain injury. Sci Rep 5, 1–10.

Hawley, ZCE, Campos-Melo, D, and Strong, MJ (2019). MiR-105 and miR-9 regulate the mRNA stability of neuronal intermediate filaments. Implications for the pathogenesis of amyotrophic lateral sclerosis (ALS). Brain Res 1706, 93–100.

He, Y, Francis, F, Myers, KA, Yu, W, Black, MM, and Baas, PW (2005). Role of cytoplasmic dynein in the axonal transport of microtubules and neurofilaments. J Cell Biol 168, 697–703.

Heins, S, Wong, PC, Muller, S, Goldie, K, Cleveland, DW, Aebi, U, Miiller, S, Goldie, K, Cleveland, DW, Aebi, U, *et al.* (1993). The Rod Domain of NF-L Determines Neurofilament Architecture, Whereas the End Domains Specify Filament Assembly and Network Formation. J Cell Biol 123, 1517–1533.

Herrmann, H, Häner, M, Brettel, M, Müller, SA, Goldie, KN, Fedtke, B, Lustig, A, Franke, WW, and Aebi, U (1996). Structure and assembly properties of the intermediate filament protein vimentin: the role of its head, rod and tail domains. J Mol Biol 264, 933–953.

Hirokawa, N (1982). Cross-linker system between neurofilaments, microtubules, and membranous organelles in frog axons revealed by the quick-freeze, deep-etching method. J Cell Biol 94, 129–142.

Hirokawa, N, Glicksman, MA, and Willard, MB (1984). Organization of mammalian neurofilament polypeptides within the neuronal cytoskeleton. J Cell Biol 98, 1523–1536.

Hisanaga, S, Gonda, Y, Inagaki, M, Ikai, A, and Hirokawa, N (1990). Effects of phosphorylation of the neurofilament L protein on filamentous structures. Cell Regul 1, 237–248.

Hisanaga, S, and Hirokawa, N (1990). Dephosphorylation-induced interactions of neurofilaments with microtubules. J Biol Chem 265, 21852–21858.

Hisanaga, S, Matsuoka, Y, Nishizawa, K, Saito, T, Inagaki, M, and Hirokawa, N (1994). Phosphorylation of native and reassembled neurofilaments composed of NF-L, NF-M, and NF-H by the catalytic subunit of cAMP-dependent protein kinase. Mol Biol Cell 5, 161–172.

Hisanaga, S-I, and Hirokawa, N (1988). Structure of the peripheral domains of neurofilaments revealed by low angle rotary shadowing. J Mol Biol 202, 297–305.

Hoffman, PN, Griffin, JW, and Price, DL (1984). Control of axonal caliber by neurofilament transport. J Cell Biol 99, 705–714.

Holmgren, A, Bouhy, D, and Timmerman, V (2012). Neurofilament phosphorylation and their proline-directed kinases in health and disease. J Peripher Nerv Syst 17, 365–376.

Huehnchen, P, Schinke, C, Bangemann, N, Dordevic, AD, Kern, J, Maierhof, SK, Hew, L, Nolte, L, Körtvelyessy, P, Göpfert, JC, *et al.* (2022). Neurofilament proteins as a potential biomarker in chemotherapy-induced polyneuropathy. JCI Insight 7, e154395.

Israeli, E, Dryanovski, DI, Schumacker, PT, Chandel, NS, Singer, JD, Julien, JP, Goldman, RD, and Opal, P (2016). Intermediate filament aggregates cause mitochondrial dysmotility and increase energy demands in giant axonal neuropathy. Hum Mol Genet 25, 2143–2157.

Jacomy, H, Zhu, Q, Couillard-Després, S, Beaulieu, J-MM, and Julien, J-PP (1999). Disruption of type IV intermediate filament network in mice lacking the neurofilament medium and heavy subunits. J Neurochem 73, 972–984.

Jayanthi, L, Stevenson, W, Kwak, Y, Chang, R, and Gebremichael, Y (2013). Conformational properties of interacting neurofilaments: Monte Carlo simulations of cylindrically grafted apposing neurofilament brushes. J Biol Phys 39, 343–362.

Jeong, S, Zhou, X, Zhulina, EB, and Jho, Y (2016). Monte Carlo Simulation of the Neurofilament Brush. Isr J Chem 56, 599–606.

Johnson-Kerner, BL, Ahmad, FS, Diaz, AG, Greene, JP, Gray, SJ, Samulski, RJ, Chung, WK, Van Coster, R, Maertens, P, Noggle, SA, *et al.* (2015). Intermediate filament protein accumulation in motor neurons derived from giant axonal neuropathy iPSCs rescued by restoration of gigaxonin. Hum Mol Genet 24, 1420–1431.

Jones, JB, and Safinya, CR (2008). Interplay between liquid crystalline and isotropic gels in self-assembled neurofilament networks. Biophys J 95, 823–835.

Kaplan, MP, Chin, SS, Fliegner, KH, and Liem, RK (1990). Alpha-internexin, a novel neuronal intermediate filament protein, precedes the low molecular weight neurofilament protein (NF-L) in the developing rat brain. J Neurosci Off J Soc Neurosci 10, 2735–2748.

Kim, S, Chang, R, Teunissen, C, Gebremichael, Y, and Petzold, A (2011). Neurofilament stoichiometry simulations during neurodegeneration suggest a remarkable self-sufficient and stable in vivo protein structure. J Neurol Sci 307, 132–138.

Koren, G, Meir, S, Holschuh, L, Mertens, HDT, Ehm, T, Yahalom, N, Golombek, A, Schwartz, T, Svergun, DI, Saleh, OA, *et al.* (2023). Intramolecular structural heterogeneity altered by long-range contacts in an intrinsically disordered protein. Proc Natl Acad Sci 120, e2220180120.

Kornreich, M, Malka-Gibor, E, Laser-Azogui, A, Doron, O, Herrmann, H, and Beck, R (2015). Composite bottlebrush mechanics: α-internexin fine-tunes neurofilament network properties. Soft Matter 11, 5839–5849.

Kornreich, M, Malka-Gibor, E, Zuker, B, Laser-Azogui, A, and Beck, R (2016). Neurofilaments Function as Shock Absorbers: Compression Response Arising from Disordered Proteins. Phys Rev Lett 117, 1–5.

Kreplak, L, Bär, H, Leterrier, JF, Herrmann, H, and Aebi, U (2005). Exploring the mechanical behavior of single intermediate filaments. J Mol Biol 354, 569–577.

Kumar, S, and Hoh, JH (2004). Modulation of repulsive forces between neurofilaments by sidearm phosphorylation. Biochem Biophys Res Commun 324, 489–496.

Kumar, S, Yin, X, Trapp, BD, Hoh, JH, and Paulaitis, ME (2002). Relating interactions between neurofilaments to the structure of axonal neurofilament distributions through polymer brush models. Biophys J 82, 2360–2372.

Kurup, N, Li, Y, Goncharov, A, and Jin, Y (2018). Intermediate filament accumulation can stabilize microtubules in Caenorhabditis elegans motor neurons. Proc Natl Acad Sci U S A 115, 3114–3119.

Kushkuley, J, Chan, WKH, Lee, S, Eyer, J, Leterrier, JF, Letournel, F, and Shea, TB (2009). Neurofilament cross-bridging competes with kinesin-dependent association of neurofilaments with microtubules. J Cell Sci 122, 3579–3586.

Kushkuley, J, Metkar, S, Chan, WKH, Lee, S, and Shea, TB (2010). Aluminum induces neurofilament aggregation by stabilizing cross-bridging of phosphorylated c-terminal sidearms. Brain Res 1322, 118–123.

Lambertsen, KL, Soares, CB, Gaist, D, and Nielsen, HH (2020). Neurofilaments: The C-reactive protein of neurology. Brain Sci 10, 1–29.

Lee, IB, Kim, SK, Chung, SH, Kim, H, Kwon, TK, Min, DS, and Chang, JS (2008). The effect of rod domain A148V mutation of neurofilament light chain on filament formation. J Biochem Mol Biol 41, 868–874.

Lee, J, Kim, S, Chang, R, Jayanthi, L, and Gebremichael, Y (2013). Effects of molecular model, ionic strength, divalent ions, and hydrophobic interaction on human neurofilament conformation. J Chem Phys 138, 015103.

Lee, S, Eyer, J, Letournel, F, Boumil, E, Hall, G, and Shea, TB (2019). Neurofilaments form flexible bundles during neuritogenesis in culture and in mature axons in situ. J Neurosci Res 97, 1306–1318.

Lee, S, Pant, HC, and Shea, TB (2014). Divergent and convergent roles for kinases and phosphatases in neurofilament dynamics. J Cell Sci 127, 4064–4077.

Lee, S, Sunil, N, and Shea, TB (2011). C-terminal neurofilament phosphorylation fosters neurofilament-neurofilament associations that compete with axonal transport. Cytoskeleton 68, 8–17.

Lee, W-C, Chen, Y-Y, Kan, D, and Chien, C-L (2012). A neuronal death model: overexpression of neuronal intermediate filament protein peripherin in PC12 cells. J Biomed Sci 19, 8.

Leermakers, FAM, and Zhulina, EB (2010). How the projection domains of NF-L and α-internexin determine the conformations of NF-M and NF-H in neurofilaments. Eur Biophys J 39, 1323–1334.

Lei, R, Lee, JP, Francis, MB, and Kumar, S (2018). Structural Regulation of a Neurofilament-Inspired Intrinsically Disordered Protein Brush by Multisite Phosphorylation. Biochemistry 57, 4019–4028.

Leterrier, JF, and Eyer, J (1987). Properties of highly viscous gels formed by neurofilaments in vitro. A possible consequence of a specific inter-filament cross-bridging. Biochem J 245, 93–101.

Leterrier, JF, Janmey, PA, and Eyer, J (2009). Microtubule-independent regulation of neurofilament interactions in vitro by neurofilament-bound ATPase activities. Biochem Biophys Res Commun 384, 37–42.

Leterrier, JF, Käs, J, Hartwig, J, Vegners, R, and Janmey, PA (1996). Mechanical effects of neurofilament cross-bridges. Modulation by phosphorylation, lipids, and interactions with F-actin. J Biol Chem 271, 15687–15694.

Li, Z, Tang, M, Liang, S, Zhang, M, Biesold, GM, He, Y, Hao, S-M, Choi, W, Liu, Y, Peng, J, *et al.* (2021). Bottlebrush polymers: From controlled synthesis, self-assembly, properties to applications. Prog Polym Sci 116, 101387.

Lin, C-H, Li, C-H, Yang, K-C, Lin, F-J, Wu, C-C, Chieh, J-J, and Chiu, M-J (2019). Blood NfL: A biomarker for disease severity and progression in Parkinson disease. Neurology 93, e1104–e1111.

Lin, Y-C, Yao, NY, Broedersz, CP, Herrmann, H, MacKintosh, FC, and Weitz, DA (2010). Origins of Elasticity in Intermediate Filament Networks. Phys Rev Lett 104, 058101.

Lu, C-H, Kalmar, B, Malaspina, A, Greensmith, L, and Petzold, A (2011). A method to solubilise protein aggregates for immunoassay quantification which overcomes the neurofilament “hook” effect. J Neurosci Methods 195, 143–150.

Lu, C-H, Macdonald-Wallis, C, Gray, E, Pearce, N, Petzold, A, Norgren, N, Giovannoni, G, Fratta, P, Sidle, K, Fish, M, *et al.* (2015). Neurofilament light chain: A prognostic biomarker in amyotrophic lateral sclerosis. Neurology 84, 2247–2257.

Malka-Gibor, E, Kornreich, M, Laser-Azogui, A, Doron, O, Zingerman-Koladko, I, Harapin, J, Medalia, O, and Beck, R (2017). Phosphorylation-Induced Mechanical Regulation of Intrinsically Disordered Neurofilament Proteins. Biophys J 112, 892–900.

Marszalek, JR, Williamson, TL, Lee, MK, Xu, Z, Hoffman, PN, Becher, MW, Crawford, TO, and Cleveland, DW (1996). Neurofilament subunit NF-H modulates axonal diameter by selectively slowing neurofilament transport. J Cell Biol 135, 711–724.

Martin, EW, and Holehouse, AS (2020). Intrinsically disordered protein regions and phase separation: sequence determinants of assembly or lack thereof. Emerg Top Life Sci 4, 307–329.

Meier, J, Couillard-Després, S, Jacomy, H, Gravel, C, and Julien, JP (1999). Extra neurofilament NF-L subunits rescue motor neuron disease caused by overexpression of the human NF-H gene in mice. J Neuropathol Exp Neurol 58, 1099—1110.

Monsma, PC, Li, Y, Fenn, JD, Jung, P, and Brown, A (2014). Local Regulation of Neurofilament Transport by Myelinating Cells. J Neurosci 34, 2979–2988.

Morris, OM, Torpey, JH, and Isaacson, RL (2021). Intrinsically disordered proteins: modes of binding with emphasis on disordered domains. Open Biol 11, 210222.

Ning, L, and Wang, B (2022). Neurofilament light chain in blood as a diagnostic and predictive biomarker for multiple sclerosis: A systematic review and meta-analysis. PLOS ONE 17, e0274565.

Ohara, O, Gahara, Y, Miyake, T, Teraoka, H, and Kitamura, T (1993). Neurofilament deficiency in quail caused by nonsense mutation in neurofilament-L gene. J Cell Biol 121, 387–395.

Ouyang, H, Nauman, E, and Shi, R (2013). Contribution of cytoskeletal elements to the axonal mechanical properties. J Biol Eng 7, 1.

Pérez-Ollé, R, López-Toledano, MA, Goryunov, D, Cabrera-Poch, N, Stefanis, L, Brown, K, and Liem, RKH (2005). Mutations in the neurofilament light gene linked to Charcot-Marie-Tooth disease cause defects in transport. J Neurochem 93, 861–874.

Perrot, R, and Julien, J-P (2011). Knockout Models of Neurofilament Proteins. In: Cytoskeleton of the Nervous System, ed. RA Nixon, and A Yuan, New York, NY: Springer, 261–277.

Petzold, A (2022). The 2022 Lady Estelle Wolfson lectureship on neurofilaments. J Neurochem 163, 179–219.

Phillips, CL, Faridounnia, M, Armao, D, and Snider, NT (2023). Stability dynamics of neurofilament and GFAP networks and protein fragments. Curr Opin Cell Biol 85, 102266.

Potokar, M, and Jorgačevski, J (2021). Plectin in the Central Nervous System and a Putative Role in Brain Astrocytes. Cells 10, 2353.

Pregent, S, Lichtenstein, A, Avinery, R, Laser-Azogui, A, Patolsky, F, and Beck, R (2015). Probing the interactions of intrinsically disordered proteins using nanoparticle tags. Nano Lett 15, 3080–3087.

Preische, O, Schultz, SA, Apel, A, Kuhle, J, Kaeser, SA, Barro, C, Gräber, S, Kuder-Buletta, E, LaFougere, C, Laske, C, *et al.* (2019). Serum neurofilament dynamics predicts neurodegeneration and clinical progression in presymptomatic Alzheimer's disease. Nat Med 25, 277–283.

Prokop, A (2020). Cytoskeletal organization of axons in vertebrates and invertebrates. J Cell Biol 219.

Puentes, F, Benkert, P, Amor, S, Kuhle, J, and Giovannoni, G (2021). Antibodies to neurofilament light as potential biomarkers in multiple sclerosis. BMJ Neurol Open 3, e000192.

Rafii, MS, Donohue, MC, Matthews, DC, Muranevici, G, Ness, S, O'Bryant, SE, and Rissman, RA (2019). Plasma Neurofilament Light and Alzheimer's Disease Biomarkers in Down Syndrome: Results from the Down Syndrome Biomarker Initiative (DSBI). J Alzheimers Dis 70, 131–138.

Rammensee, S, Janmey, PA, and Bausch, AR (2007). Mechanical and structural properties of in vitro neurofilament hydrogels. Eur Biophys J 36, 661–668.

Rao, MV, Campbell, J, Yuan, A, Kumar, A, Gotow, T, Uchiyama, Y, and Nixon, RA (2003). The neurofilament middle molecular mass subunit carboxyl-terminal tail domains is essential for the radial growth and cytoskeletal architecture of axons but not for regulating neurofilament transport rate. J Cell Biol 163, 1021–1031.

Rao, MV, Darji, S, Stavrides, PH, Goulbourne, CN, Kumar, A, Yang, DS, Yoo, L, Peddy, J, Lee, JH, Yuan, A, *et al.* (2022). Autophagy is a novel pathway for neurofilament protein degradation in vivo. Autophagy.

Rao, MV, Garcia, ML, Miyazaki, Y, Gotow, T, Yuan, A, Mattina, S, Ward, CM, Calcutt, NA, Uchiyama, Y, Nixon, RA, *et al.* (2002). Gene replacement in mice reveals that the heavily phosphorylated tail of neurofilament heavy subunit does not affect axonal caliber or the transit of cargoes in slow axonal transport. J Cell Biol 158, 681–693.

Rao, MV, Houseweart, MK, Williamson, TL, Crawford, TO, Folmer, J, and Cleveland, DW (1998). Neurofilament-dependent radial growth of motor axons and axonal organization of neurofilaments does not require the neurofilament heavy subunit (NF-H) or its phosphorylation. J Cell Biol 143, 171–181.

Rebelo, AP, Abrams, AJ, Cottenie, E, Horga, A, Gonzalez, M, Bis, DM, Sanchez-Mejias, A, Pinto, M, Buglo, E, Markel, K, *et al.* (2016). Cryptic Amyloidogenic Elements in the 3′ UTRs of Neurofilament Genes Trigger Axonal Neuropathy. Am J Hum Genet 98, 597–614.

Renganathan, B, Zewe, JP, Cheng, Y, Paumier, J-M, Kittisopikul, M, Ridge, KM, Opal, P, and Gelfand, VI (2023). Gigaxonin is required for intermediate filament transport. FASEB J 37.

Rudrabhatla, P, Jaffe, H, and Pant, HC (2011). Direct evidence of phosphorylated neuronal intermediate filament proteins in neurofibrillary tangles (NFTs): phosphoproteomics of Alzheimer's NFTs. FASEB J 25, 3896–3905.

Sainio, MT, Ylikallio, E, Mäenpää, L, Lahtela, J, Mattila, P, Auranen, M, Palmio, J, and Tyynismaa, H (2018). Absence of NEFL in patient-specific neurons in early-onset Charcot-Marie-Tooth neuropathy. Neurol Genet 4.

Sasaki, T, Gotow, T, Shiozaki, M, Sakaue, F, Saito, T, Julien, J-P, Uchiyama, Y, and Hisanaga, S-I (2006). Aggregate formation and phosphorylation of neurofilament-L Pro22 Charcot–Marie–Tooth disease mutants. Hum Mol Genet 15, 943–952.

Scott, D, Smith, KE, O'Brien, BJ, and Angelides, KJ (1985). Characterization of mammalian neurofilament triplet proteins: Subunit stoichiometry and morphology of native and reconstituted filaments. J Biol Chem 260, 10736–10747.

Shah, JV, Flanagan, LA, Janmey, PA, and Leterrier, J-F (2000). Bidirectional Translocation of Neurofilaments along Microtubules Mediated in Part by Dynein/Dynactin. Mol Biol Cell 11, 3495–3508.

Sharma, S, Mücke, N, Katus, HA, Herrmann, H, and Bär, H (2009). Disease mutations in the "head" domain of the extra-sarcomeric protein desmin distinctly alter its assembly and network-forming properties. J Mol Med 87, 1207–1219.

Shea, TB, and Lee, S (2011). Neurofilament phosphorylation regulates axonal transport by an indirect mechanism: A merging of opposing hypotheses. Cytoskeleton 68, 589–595.

Snider, NT, and Omary, MB (2014). Post-translational modifications of intermediate filament proteins: mechanisms and functions. Nat Rev Mol Cell Biol 15, 163–177.

Srinivasan, N, Bhagawati, M, Ananthanarayanan, B, and Kumar, S (2014). Stimuli-sensitive intrinsically disordered protein brushes. Nat Commun 5, 1–8.

Stevenson, W, Chang, R, and Gebremichael, Y (2011). Phosphorylation-mediated conformational changes in the mouse neurofilament architecture: Insight from a neurofilament brush model. J Mol Biol 405, 1101–1118.

Stone, EJ, Kolb, SJ, and Brown, A (2021). A review and analysis of the clinical literature on Charcot–Marie–Tooth disease caused by mutations in neurofilament protein L. Cytoskeleton 78, 97–110.

Stone, EJ, Uchida, A, and Brown, A (2019). Charcot-Marie-Tooth Disease Type 2E/1F Mutant Neurofilament Proteins Assemble into Neurofilaments. Cytoskelet Hoboken NJ 76, 423.

Straube-West, K, Loomis, PA, Opal, P, and Goldman, RD (1996). Alterations in neural intermediate filament organization: Functional implications and the induction of pathological changes related to motor neuron disease. J Cell Sci 109, 2319–2329.

Stys, PK, and Jiang, Q (2002). Calpain-dependent neurofilament breakdown in anoxic and ischemic rat central axons. Neurosci Lett 328, 150–154.

Sunil, N, Lee, S, and Shea, TB (2012). Interference with kinesin-based anterograde neurofilament axonal transport increases neurofilament-neurofilament bundling. Cytoskeleton 69, 371–379.

Trojanowski, JQ, and Lee, VM-Y (1998). Aggregation of Neurofilament and α-Synuclein Proteins in Lewy Bodies: Implications for the Pathogenesis of Parkinson Disease and Lewy Body Dementia. Arch Neurol 55, 151–152.

Uchida, A, Alami, NH, and Brown, A (2009). Tight functional coupling of kinesin-1A and dynein motors in the bidirectional transport of neurofilaments. Mol Biol Cell 20, 4997–5006.

Uchida, A, Colakoglu, G, Wang, L, Monsma, PC, and Brown, A (2013). Severing and end-to-end annealing of neurofilaments in neurons. Proc Natl Acad Sci U S A 110, E2696.

Uchida, A, Peng, J, and Brown, A (2023). Regulation of neurofilament length and transport by a dynamic cycle of phospho-dependent polymer severing and annealing. Mol Biol Cell 34.

Uchida, A, Tashiro, T, Komiya, Y, Yorifuji, H, Kishimoto, T, and Hisanaga, SI (2004). Morphological and biochemical changes of neurofilaments in aged rat sciatic nerve axons. J Neurochem 88, 735–745.

Uchida, A, Yorifuji, H, Lee, VM -Y., Kishimoto, T, and Hisanaga, S (1999). Neurofilaments of aged rats: The strengthened interneurofilament interaction and the reduced amount of NF-M. J Neurosci Res 58, 337–348.

Uchikado, H, Li, A, Lin, W-L, and Dickson, DW (2006). Heterogeneous inclusions in neurofilament inclusion disease. Neuropathology 26, 417–421.

Uversky, VN (2021). Recent Developments in the Field of Intrinsically Disordered Proteins: Intrinsic Disorder-Based Emergence in Cellular Biology in Light of the Physiological and Pathological Liquid-Liquid Phase Transitions. Annu Rev Biophys 50, 135–156.

Veeranna, Yang, D-S, Lee, J-H, Vinod, KY, Stavrides, P, Amin, ND, Pant, HC, and Nixon, RA (2011). Declining phosphatases underlie aging-related hyperphosphorylation of neurofilaments. Neurobiol Aging 32, 2016–2029.

Verduzco, R, Li, X, Pesek, SL, and Stein, GE (2015). Structure, function, self-assembly, and applications of bottlebrush copolymers. Chem Soc Rev 44, 2405–2420.

Vohnoutka, RB, Boumil, EF, Liu, Y, Uchida, A, Pant, HC, and Shea, TB (2017). Influence of a GSK3β phosphorylation site within the proximal C-terminus of Neurofilament-H on neurofilament dynamics. Biol Open 6, 1516–1527.

Wagner, OI, Ascaño, J, Tokito, M, Leterrier, J-F, Janmey, PA, and Holzbaur, ELF (2004). The Interaction of Neurofilaments with the Microtubule Motor Cytoplasmic Dynein. Mol Biol Cell 15, 5092–5100.

Wagner, OI, Rammensee, S, Korde, N, Wen, Q, Leterrier, JF, and Janmey, PA (2007). Softness, strength and self-repair in intermediate filament networks. Exp Cell Res 313, 2228–2235.

Wang, L, Ho, C, Sun, D, Liem, RKH, and Brown, A (2000). Rapid movement of axonal neurofilaments interrupted by prolonged pauses. Nat Cell Biol 2, 137–141.

Wiche, G (2021). Plectin-mediated intermediate filament functions: Why isoforms matter. Cells 10, 2154.

Willard, M, and Simon, C (1981). Antibody decoration of neurofilaments. J Cell Biol 89, 198–205.

Wong, NKY, He, BP, Strong, MJ, NK, W, BP, H, MJ, S, Wong, NKY, He, BP, and Strong, MJ (2000). Characterization of neuronal intermediate filament protein expression in cervical spinal motor neurons in sporadic amyotrophic lateral sclerosis (ALS). J Neuropathol Exp Neurol 59, 972–982.

Xia, C-H, Roberts, EA, Her, L-S, Liu, X, Williams, DS, Cleveland, DW, and Goldstein, LSB (2003). Abnormal neurofilament transport caused by targeted disruption of neuronal kinesin heavy chain KIF5A. J Cell Biol 161, 55–66.

Xu, Z, Marszalek, JR, Lee, MK, Wong, PC, Folmer, J, Crawford, TO, Hsieh, ST, Griffin, JW, and Cleveland, DW (1996). Subunit composition of neurofilaments specifies axonal diameter. J Cell Biol 133, 1061–1069.

Yabe, JT, Chylinski, T, Wang, F-S, Pimenta, A, Kattar, SD, Linsley, M-D, Chan, WK-H, and Shea, TB (2001). Neurofilaments Consist of Distinct Populations That Can Be Distinguished by C-Terminal Phosphorylation, Bundling, and Axonal Transport Rate in Growing Axonal Neurites. J Neurosci 21, 2195–2205.

Yabe, JT, Jung, C, Chan, WK-H, and Shea, TB (2000). Phospho-dependent association of neurofilament proteins with kinesin in situ. Cell Motil 45, 249–262.

Yadav, P, Selvaraj, BT, Bender, FLP, Behringer, M, Moradi, M, Sivadasan, R, Dombert, B, Blum, R, Asan, E, Sauer, M, *et al.* (2016). Neurofilament depletion improves microtubule dynamics via modulation of Stat3/stathmin signaling. Acta Neuropathol (Berl) 132, 93–110.

Yamada, KM, Spooner, BS, and Wessells, NK (1971). Ultrastructure and function of growth cones and axons of cultured nerve cells. J Cell Biol 49, 614–635.

Yamasaki, H, Itakura, C, and Mizutani, M (1991). Hereditary hypotrophic axonopathy with neurofilament deficiency in a mutant strain of the Japanese quail. Acta Neuropathol (Berl) 82, 427–434.

Yan, Y, Jensen, K, and Brown, A (2007). The polypeptide composition of moving and stationary neurofilaments in cultured sympathetic neurons. Cell Motil 64, 299–309.

Yang, B, Liu, Z, Liu, H, and Nash, MA (2020). Next Generation Methods for Single-Molecule Force Spectroscopy on Polyproteins and Receptor-Ligand Complexes. Front Mol Biosci 7, 85.

Yang, Y, Dowling, J, Yu, QC, Kouklis, P, Cleveland, DW, and Fuchs, E (1996). An essential cytoskeletal linker protein connecting actin microfilaments to intermediate filaments. Cell 86, 655–665.

Yao, NY, Braedersz, CP, Lin, YC, Kasza, KE, MacKintosh, FC, and Weitz, DA (2010). Elasticity in Ionically cross-linked neurofilament networks. Biophys J 98, 2147–2153.

Yin, X, Crawford, TO, Griffin, JW, Tu, P, Lee, VM-Y, Li, C, Roder, J, and Trapp, BD (1998). Myelin-Associated Glycoprotein Is a Myelin Signal that Modulates the Caliber of Myelinated Axons. J Neurosci 18, 1953–1962.

Yokokura, TJ, Duan, C, Ding, EA, Kumar, S, and Wang, R (2023). Effects of Ionic Strength on the Morphology, Scattering, and Mechanical Response of Neurofilament-Derived Protein Brushes. Biomacromolecules 25, 328–337.

Yuan, A, Hassinger, L, Rao, MV, Julien, JP, Miller, CCJ, and Nixon, RA (2015a). Dissociation of axonal neurofilament content from its transport rate. PLoS ONE 10, e0133848.

Yuan, A, and Nixon, RA (2021). Neurofilament Proteins as Biomarkers to Monitor Neurological Diseases and the Efficacy of Therapies. Front Neurosci 15.

Yuan, A, and Nixon, RA (2023). Posttranscriptional regulation of neurofilament proteins and tau in health and disease. Brain Res Bull 192, 115–127.

Yuan, A, Rao, MV, Sasaki, T, Chen, Y, Kumar, A, Veeranna, Liem, RKH, Eyer, J, Peterson, AC, Julien, JP, *et al.* (2006). α-internexin is structurally and functionally associated with the neurofilament triplet proteins in the mature CNS. J Neurosci 26, 10006–10019.

Yuan, A, Rao, MV, Veeranna, and Nixon, RA (2017). Neurofilaments and Neurofilament Proteins in Health and Disease. Cold Spring Harb Perspect Biol 9.

Yuan, A, Sasaki, T, Kumar, A, Peterhoff, CM, Rao, MV, Liem, RK, Julien, JP, and Nixon, RA (2012). Peripherin is a subunit of peripheral nerve neurofilaments: Implications for differential vulnerability of cns and peripheral nervous system axons. J Neurosci 32, 8501–8508.

Yuan, A, Sershen, H, Veeranna, Basavarajappa, BS, Kumar, A, Hashim, A, Berg, M, Lee, JH, Sato, Y, Rao, MV, *et al.* (2015b). Neurofilament subunits are integral components of synapses and modulate neurotransmission and behavior in vivo. Mol Psychiatry 20, 986–994.

Zhai, J, Lin, H, Julien, JP, and Schlaepfer, WW (2007). Disruption of neurofilament network with aggregation of light neurofilament protein: A common pathway leading to motor neuron degeneration due to Charcot-Marie-Tooth disease-linked mutations in NFL and HSPB1. Hum Mol Genet 16, 3103–3116.

Zhao, J, Brown, K, and Liem, RKH (2017). Abnormal neurofilament inclusions and segregations in dorsal root ganglia of a Charcot-Marie-Tooth type 2E mouse model. PLOS ONE 12, e0180038.

Zheng, YL, Li, BS, Veeranna, and Pant, HC (2003). Phosphorylation of the head domain of neurofilament protein (NF-M). A factor regulating topographic phosphorylation of NF-M tail domain KSP sites in neurons. J Biol Chem 278, 24026–24032.

Zhou, X, Kato, M, and McKnight, SL (2023). How do disordered head domains assist in the assembly of intermediate filaments? Curr Opin Cell Biol 85, 102262.

Zhou, X, Lin, Y, Kato, M, Mori, E, Liszczak, G, Sutherland, L, Sysoev, VO, Murray, DT, Tycko, R, and McKnight, SL (2021). Transiently structured head domains control intermediate filament assembly. Proc Natl Acad Sci U S A 118, e2022121118.

Zhou, X, Sumrow, L, Tashiro, K, Sutherland, L, Liu, D, Qin, T, Kato, M, Liszczak, G, and McKnight, SL (2022). Mutations linked to neurological disease enhance self-association of low-complexity protein sequences. Science 377, eabn5582.

Zhu, Q, Couillard-Després, S, and Julien, JP (1997). Delayed maturation of regenerating myelinated axons in mice lacking neurofilaments. Exp Neurol 148, 299–316.

Zhulina, EB, and Leermakers, FAM (2007). Effect of the ionic strength and pH on the equilibrium structure of a neurofilament brush. Biophys J 93, 1452–1463.

Zhulina, EB, and Leermakers, FAM (2009). On the polyelectrolyte brush model of neurofilaments. Soft Matter 5, 2836–2840.

Zhulina, EB, and Leermakers, FAM (2010). The polymer brush model of neurofilament projections: Effect of protein composition. Biophys J 98, 462–469.

Zmira, O, Halpern, AI, and Drori, T (2020). Anti-neurofilament antibodies and neurodegeneration: Markers and generators. J Neuroimmunol 344, 577248.

Zucchi, E, Bonetto, V, Sorarù, G, Martinelli, I, Parchi, P, Liguori, R, and Mandrioli, J (2020). Neurofilaments in motor neuron disorders: towards promising diagnostic and prognostic biomarkers. Mol Neurodegener 15, 58.

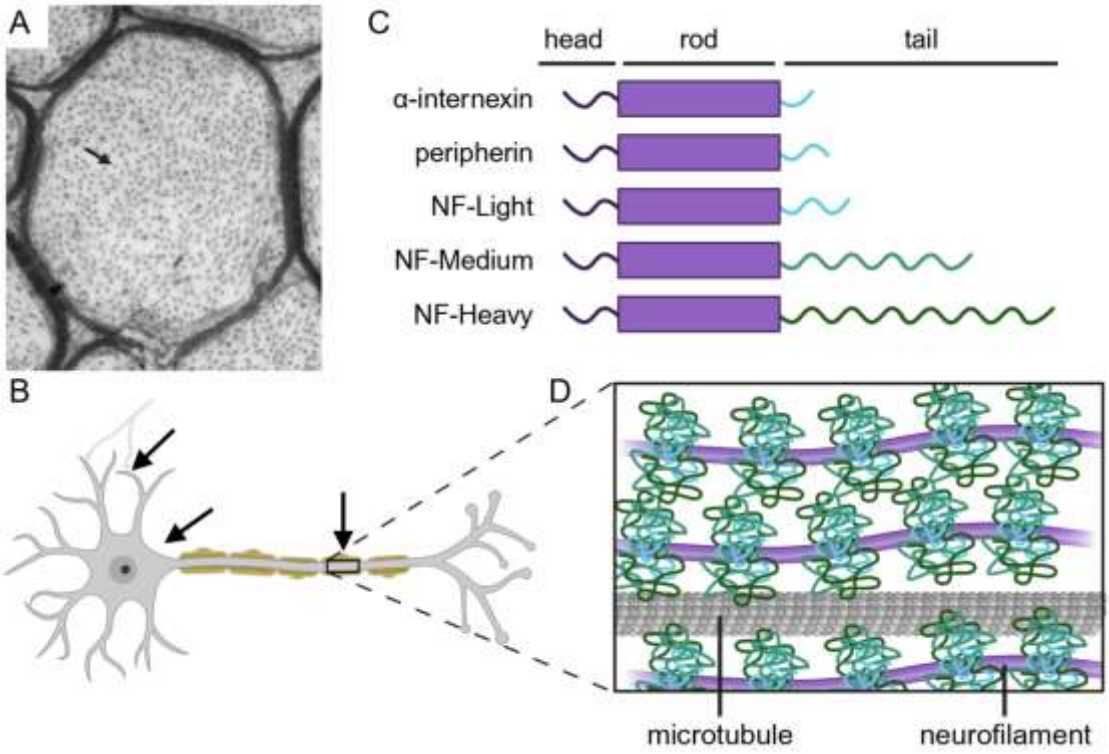

Figure Legends

Figure 1: Localization and composition of axonal NFs. (A) Electron micrograph of a cross-section of distal region of mouse optic nerve, adapted from (Yuan *et al.*, 2015a). NF cores appear as distributed dark points (arrow). (B) NF localization within a neuron at synapses, in the soma, and in the axon (arrows). (C) Schematics of the NF subunit protein domains. (D) Diagram of assembled NFs filling the axon along with microtubules. Figure created with BioRender.com.

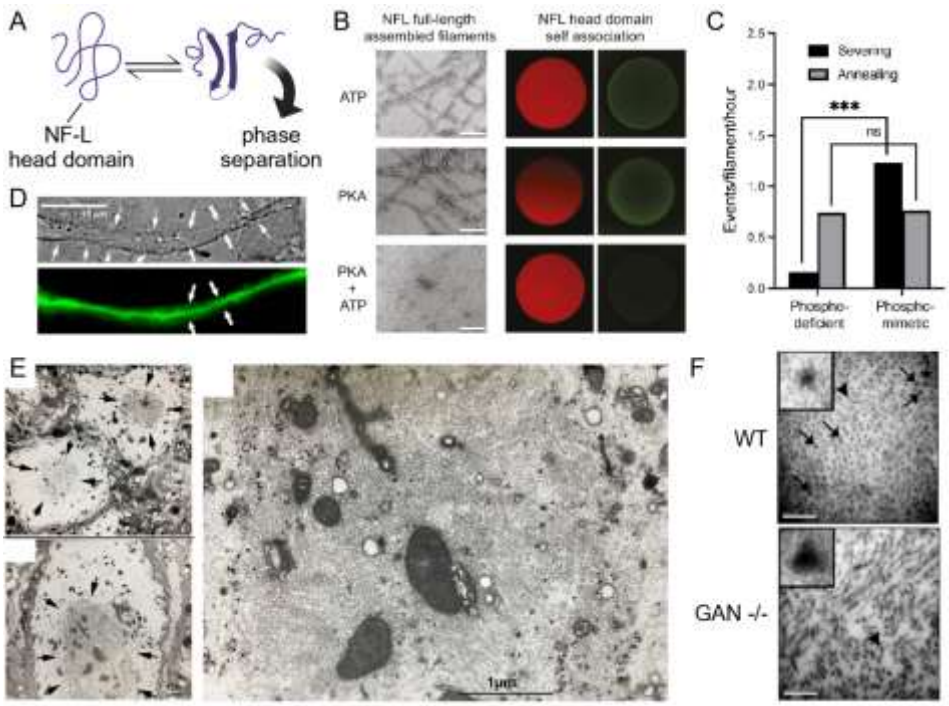

Figure 2: Regulation of NF assembly and bundled or aggregated NF ultrastructures. (A) The NF-L head domain takes on a transient cross-beta structure, enabling phase separation. (B) Filament assembly (left), as well as colocalization between mCherry-tagged (center) and GFP-tagged (right) NF-L head domains, are ablated after phosphorylation by protein kinase A (PKA). Reproduced from (Zhou *et al.*, 2021). (C) Head-domain phosphodeficient NF-L is less frequently severed than phosphomimetic NFL in cultured neurons. Reproduced from (Uchida *et al.*, 2023). (D) Phase-contrast (top) and fluorescence (bottom) micrographs of a neurite of a neuroblastoma cell expressing NFH-GFP fusion protein, reproduced from (Boumil *et al.*, 2018). Arrows indicate neurite size; NF "bundle" is visible as a central region of high NFH density within the neurite. (E) Left: Bundled NF ultrastructures (arrows) in regenerating lamprey neurons. Right: higher-magnification view of bundled NFs, showing dense filament packing and variety of orientations. Scale bars 1 μm. Adapted from (Lee *et al.*, 2019). (F) Electron micrographs of axons from wild type (top) or giant axonal neuropathy model mice (bottom), showing altered NF orientation and size. Arrows indicate microtubules, arrowheads indicate single NFs shown in higher-magnification insets. Scale bars 200 nm. Adapted from (Ganay *et al.*, 2011). Figure created with BioRender.com.

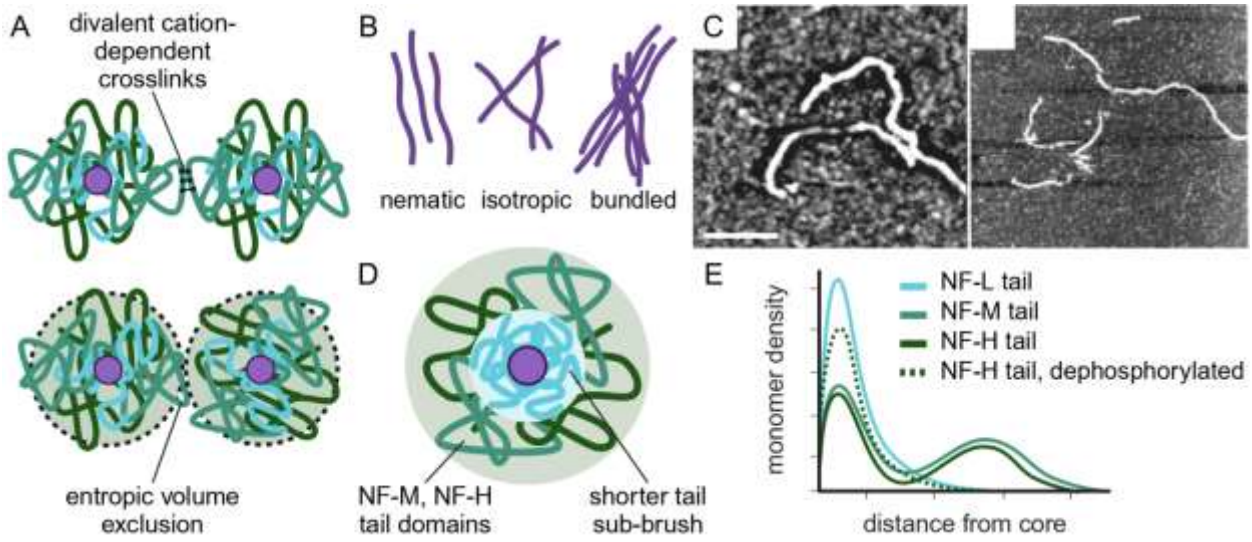

Figure 3: Inter-filament interaction models and NF tail domain conformations. (A) Diagrams of two models of inter-filament interaction: divalent cation based crosslinking and entropic volume exclusion. (B) Diagrams of structures in liquid crystal hydrogel phases from (Deek *et al.*, 2016). (C) Left: native NFs with excluded volume; right: NF-L only reconstituted NFs with no excluded volume. Scale bar 500 nm. Reproduced from (Brown and Hoh, 1997), copyright 1997 American Chemical Society. (D) Schematic of NF tail brush structure, showing sub-brush formed of shorter tailed proteins such as NF-L. (E) Example brush substructures and subunit localizations accessible by simulation or theoretical modeling. Results qualitatively adapted from (Zhulina and Leermakers, 2007) and (Lee *et al.*, 2013). Figure created with BioRender.com.

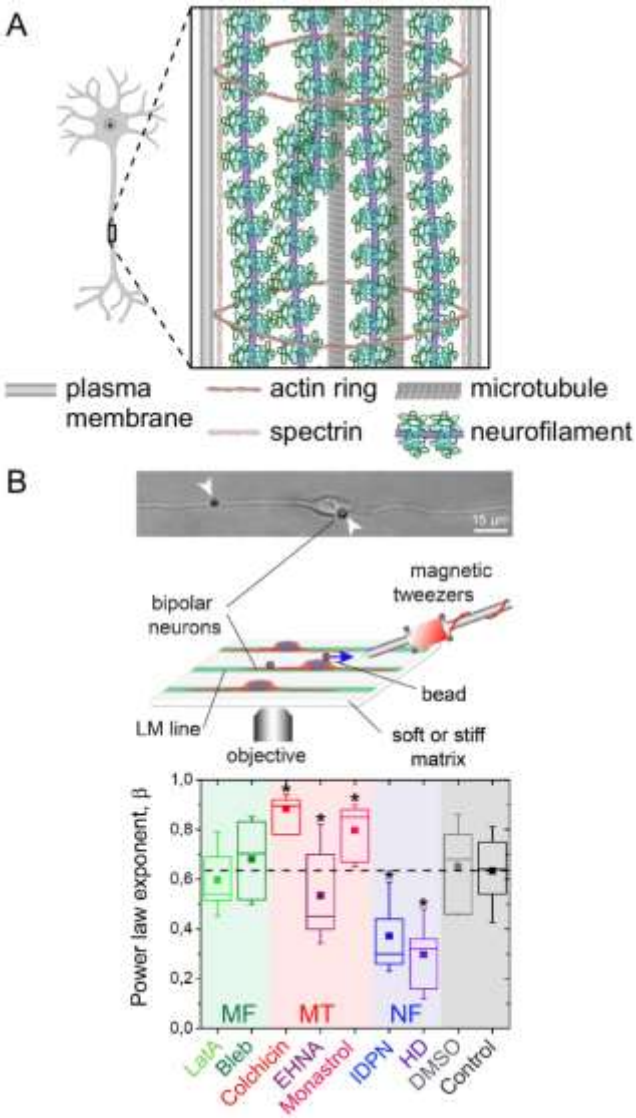

Figure 4: NFs in axon mechanics. (A) Simplified schematic of the axonal cytoskeleton including NFs, microtubules, and membrane-associated periodic scaffold including actin rings and spectrin. (B) Top: magnetic tweezers were used to pull a fibronectin-coated bead to measure cell mechanical properties at the neurite. Bottom: Neurite viscoelasticity decreases when treated with the compounds IDPN and 2,5-hexanedione (HD), which disrupt NF organization. Reproduced from (Grevesse *et al.*, 2015). Figure created with BioRender.com.

Tables

Table 1: Effects of NF subunit proteins on inter-NF spacing and tail domain brush conformations.

Platform	NF-NF Spacing or Brush Size (nm) [a]	Role of subunit in spacing or brush size			References
		α-internexin	NF-M	NF-H	
Mice	Spacing: ~45			Does not affect spacing	(Rao *et al.*, 2002)
Mice	Spacing: WT ~45 NF-M tail deleted ~39 NF-M/NF-H tails deleted ~30		Increases spacing		(Garcia *et al.*, 2003; Rao *et al.*, 2003)
Mice	Spacing: WT ~30 NF-M phospho-incompetent tail ~25 but distribution overlaps		NF-M phosphorylation does not affect spacing		(Garcia *et al.*, 2009)
Hydrogel SAXS			Promotes more nematic gel phases than NF-H	Promotes isotropic gel formation more than NF-M	(Jones and Safinya, 2008; Deek *et al.*, 2013)
Hydrogel SAXS	Spacing: 80 (low pressure) 40 (high pressure)			Increases spacing more than NF-M	(Beck *et al.*, 2010b)
Hydrogel SAXS	Spacing, α-internexin/ NF-L/NF-M/NF-H quadruplet: 80 (low pressure) 25 (high pressure)	Increases spacing compared to NF-L, only if NF-M present			(Kornreich *et al.*, 2015)
Hydrogel SAXS				Increases spacing if NF-M is also present	(Deek *et al.*, 2016)
Hydrogel SAXS	Spacing: 80 (low pressure) 30 (high pressure)		NF-M phosphorylation decreases spacing	NF-H phosphorylation increases spacing	(Malka-Gibor *et al.*, 2017)
AFM imaging	Exclusion zone size: ~50-100		No exclusion zone when NF-M and NF-H removed	No exclusion zone when NF-M and NF-H removed	(Brown and Hoh, 1997)
Grafted recomb-inant NF-H tail				Expands upon phosphorylation	(Srinivasan *et al.*, 2014; Lei *et al.*, 2018)
SCFT	Brush height: ~40			Expands upon phosphorylation to join NF-M at the brush periphery	(Zhulina and Leermakers, 2007)
SCFT	Brush heights: ~45 within a range of stoichiometries, strongly dependent on phosphorylation level				(Zhulina and Leermakers, 2010)
SCFT	Brush heights: NF-L/NF-M/NF-H: ~45 α-internexin/ NF-L/NF-M/NF-H: ~45 α-internexin/NF-M/NF-H: ~40	Decreases brush size compared to NF-L due to less repulsion of NF-M or phospho-NF-H			(Leermakers and Zhulina, 2010)
Simulation				Expands upon phosphorylation, but still not as extended as NF-M	(Chang *et al.*, 2009)
Simulation	Brush height: ~60			Slightly more extended than NF-M at high ionic strength	(Jayanthi *et al.*, 2013; Lee *et al.*, 2013)

[a] Spacing and brush sizes for non-mouse studies are given for phosphorylated proteins, 100-200 mM solution ionic strength, and compositions including NF-L, NF-M, and NF-H tail proteins as well as α-internexin when noted.